Electronic Supplementary Information (ESI) for

A Grafted Flame-retardant Gel Polymer Electrolyte Stabilizing Lithium Metal for High-safety Lithium Metal Battery

*Shaoshan Chen [a], Yong Wang [a], Zhongxiu Li [a], Yiyui Feng [a] and Wei Feng [a,b] **

[a]School of Materials Science and Engineering, Tianjin University, Tianjin 300072, P. R. China

[b]Key Laboratory of Advanced Ceramics and Machining Technology Ministry of Education, Tianjin 300072, P. R. China

*Corresponding authors: weifeng@tju.edu.cn

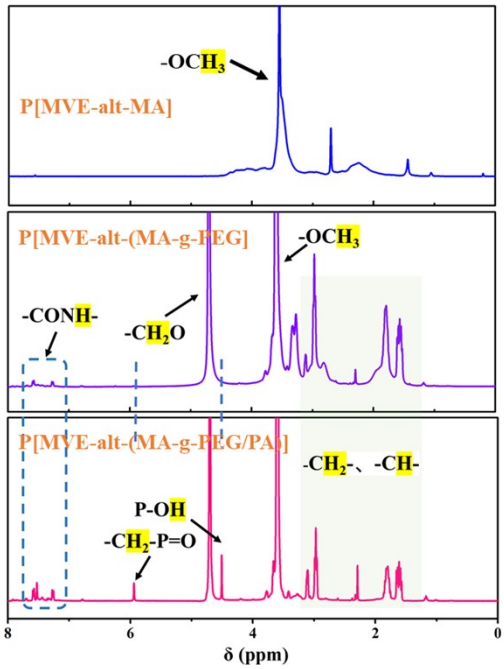

Figure S1 The ^{1}H NMR spectrum of P[MVE-alt-MA], P[MVE-alt-(MA-g-PEG] and P[MVE-alt-(MA-g-PEG/PA)]

In comparison with P[MVE-alt-MA], P[MVE-alt-(MA-g-PEG)] exhibited characteristic peaks of -CH_2O (4.7 ppm) and -CONH- (7.2~7.7 ppm), confirming the grafting of the NH_2-PEG-NH_2.

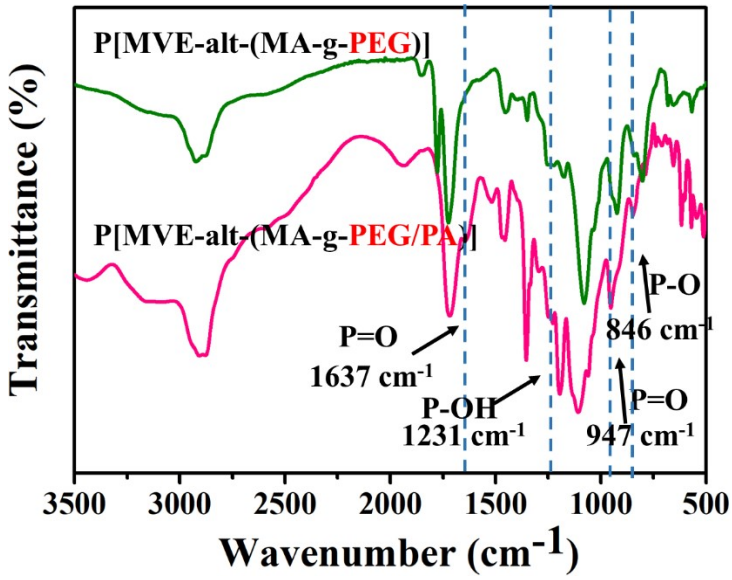

Figure S2 The FT-IR spectrum of P[MVE-alt-(MA-g-PEG)] and P[MVE-alt-(MA-g-PEG/PA)]

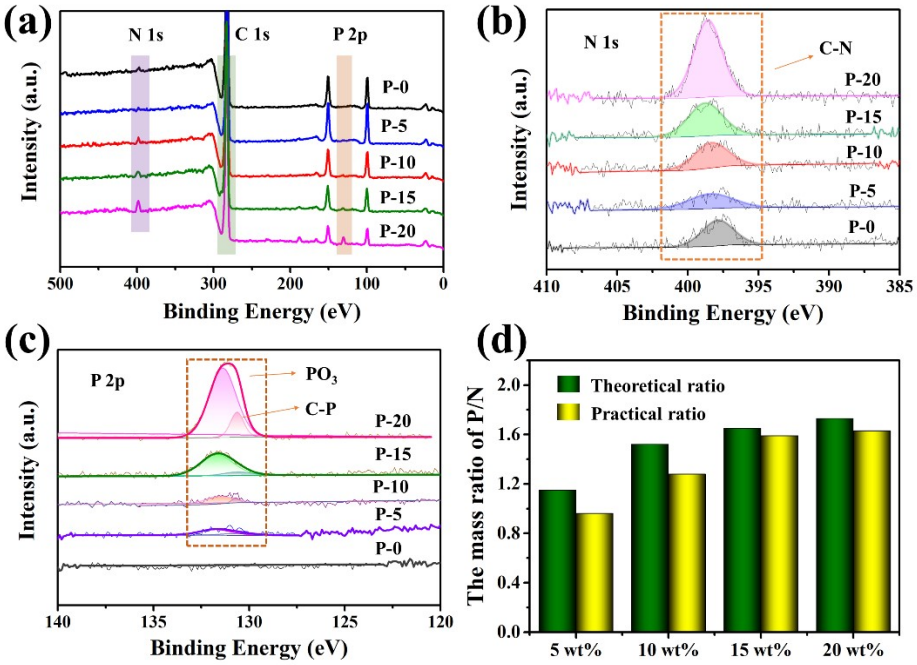

Figure S3 (a) XPS spectra, (b) N1s spectra and (c) P 2p spectra of P-0, 5, 10, 15 and 20. (d) Theoretical and practical mass ratios of P/N elements in P-0, 5, 10, 15 and 20

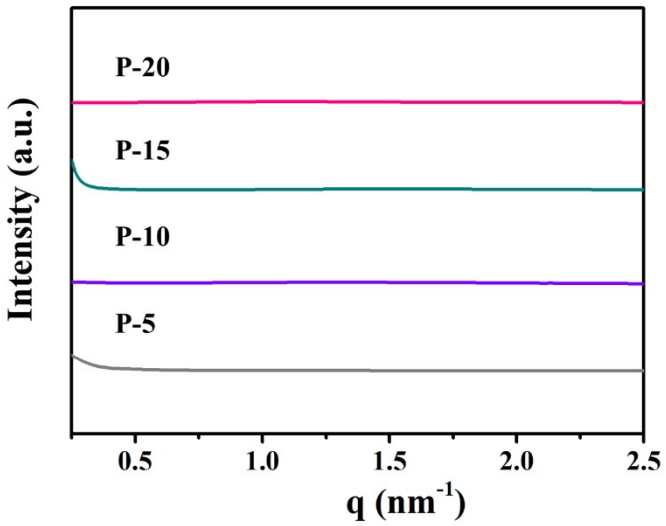

Figure S4 SAXS spectra of P-5, 10, 15 and 20

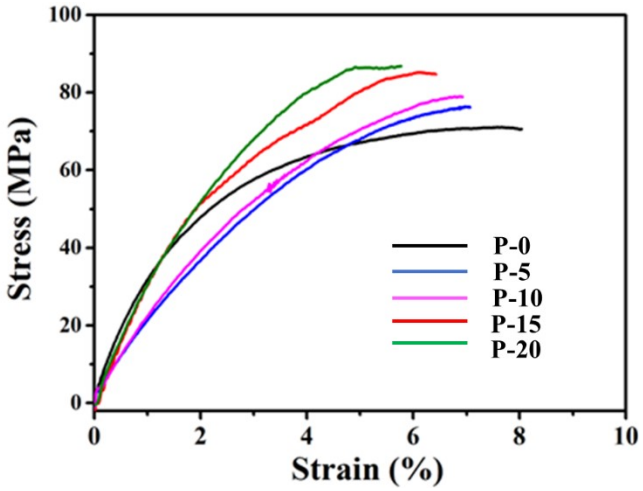

Figure S5 The stress-strain curves of different P[MVE-alt-(MA-g-PEG/PA)] films

The stress-strain profiles of different P[MVE-alt-(MA-g-PEG/PA)] films are shown in FigureS4. With the increase of 3-APPA, there is a decrease in percentage of breaking elongation and an increase in tensile strength.

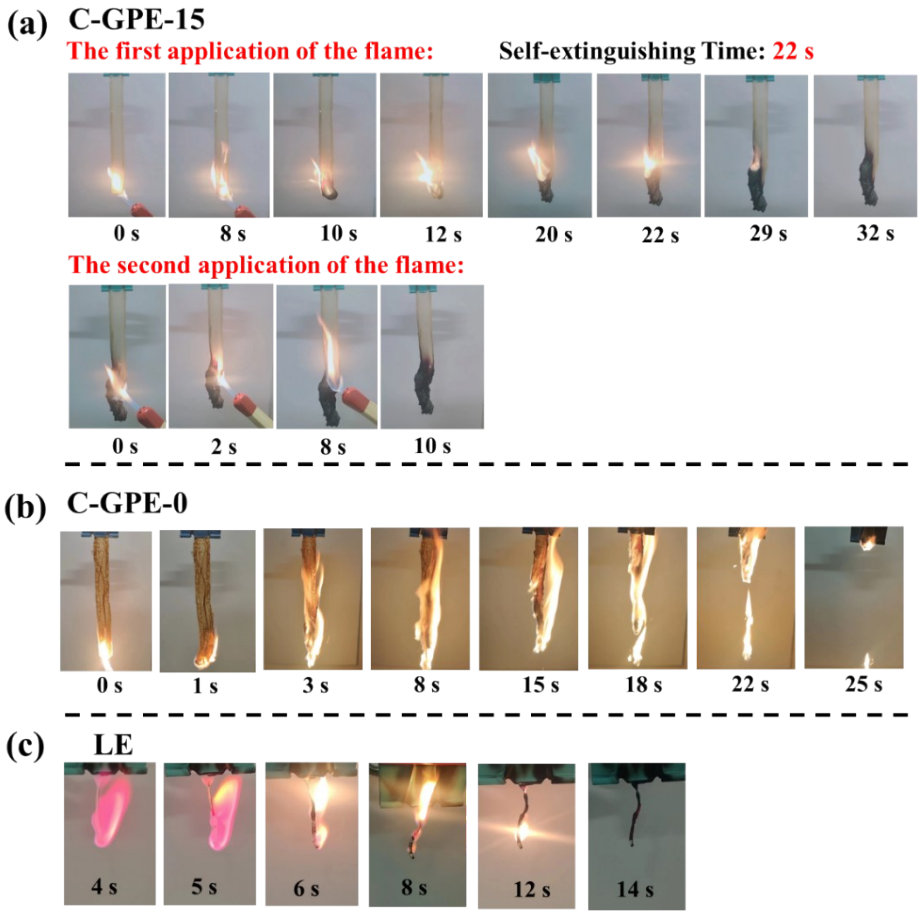

Figure S6. Video screenshots of C-GPE-15, C-GPE-0 and LE during the UL-94 test

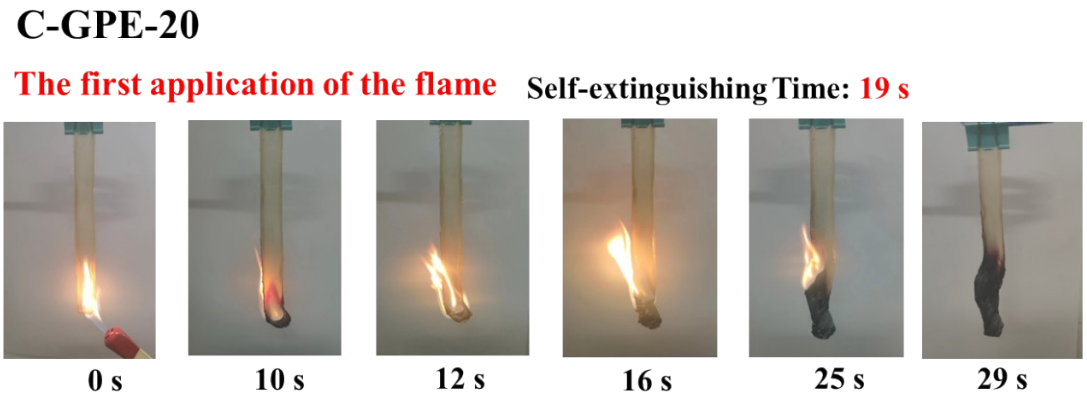

Figure S7 Video screenshots of C-GPE-20 during the UL-94 test

Table S1 Summary of Flame Retardancy Grades of C-GPE

Sample	t_1	t_2	UL-94 grade
Standard-1	≤10 s	≤30 s	V-0
Standard-2	≤30 s	≤60 s	V-1
C-GPE-15	22 s	/	V-1
C-GPE-20	19 s	/	V-1

t_1 was flame duration of the first application of the flame.

t_2 was flame duration of the second application of the flame.

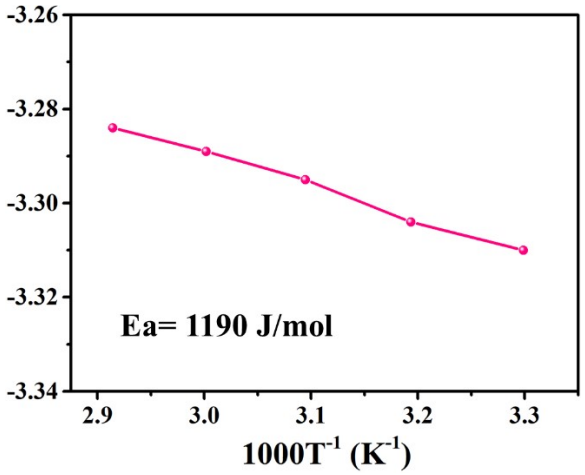

Figure S8 Fitting curve of the Arrhenius equation about σ_{Li+} and temperature for C-GPE-15

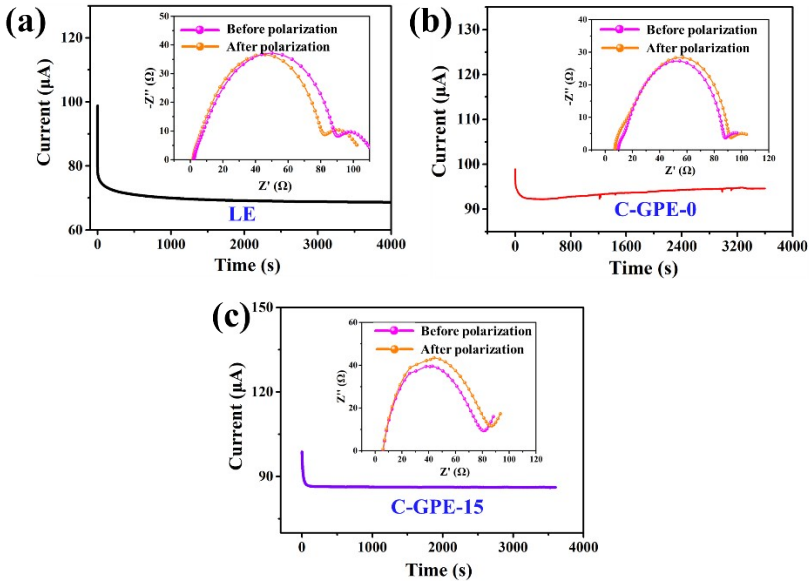

Figure S9 Polarization curves and EIS plots before and after polarization of LE, C-GPE-0 and C-GPE-15 at 30 ℃

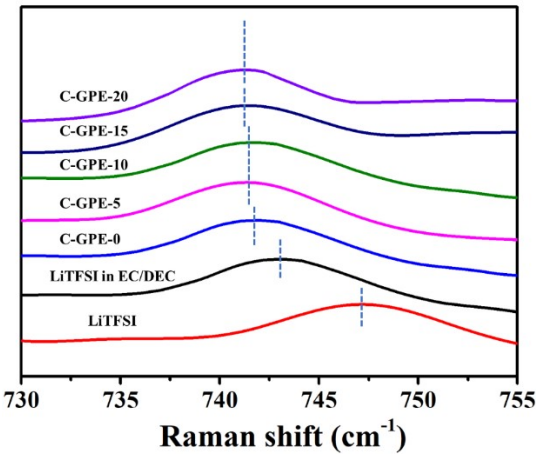

Figure S10 The Raman curves of LiTFSI, LiTFSI in EC/DEC, C-GPE-0, C-GPE-5, C-GPE-10, C-GPE-15 and C-GPE-20

The Raman spectrum observed between 730 and 755 cm^{-1} corresponds to the vibrational modes of TFSI- (including S – N stretching, C – S stretching, and CF_3 bending), where bands at 740 and 747 cm^{-1} were assigned to free $TFSI^-$ and coordinated $TFSI^-$, respectively **[1]**. With the grafting 0f PEG and 3-APPA, the Raman peak of the electrolyte shifts to the low shift, which means that there is more free TFSI- in the electrolytes.

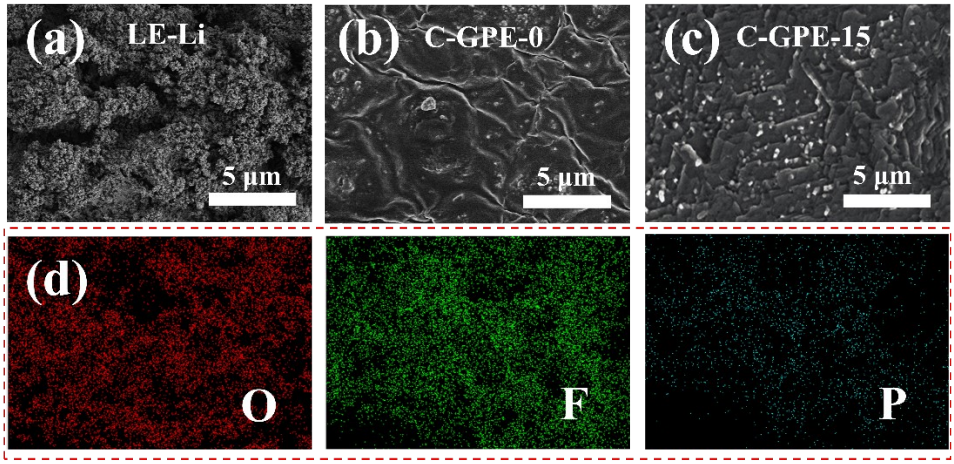

Figure S11 SEM images of Li anode in Li symmetrical cells with LE, C-GPE-0 and C-GPE-15 after 100 h; (h) EDS mapping of the SEM images of the Li surface collected from Li|C-GPE-15|Li after 100 h

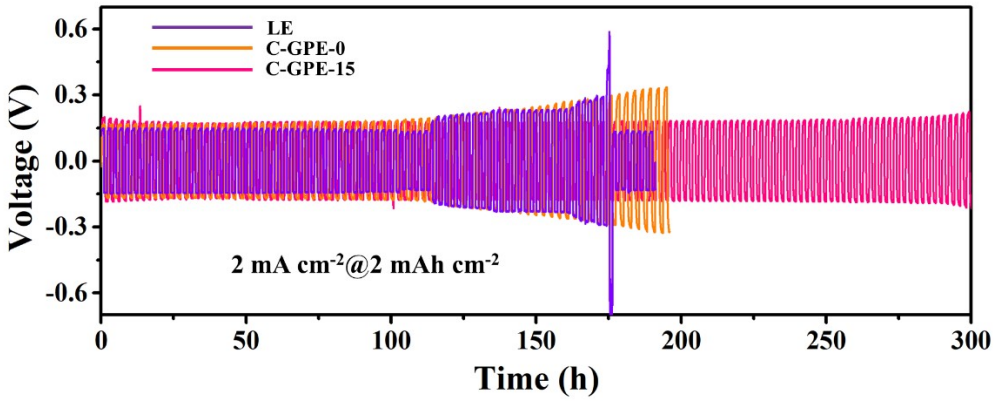

Figure S12 Galvanostatic plating/stripping curves of Li symmetrical cells with LE, C-GPE-0 and C-GPE-15 at 2 mA cm^{-2}@2 mAh cm^{-2} upon 30 °C

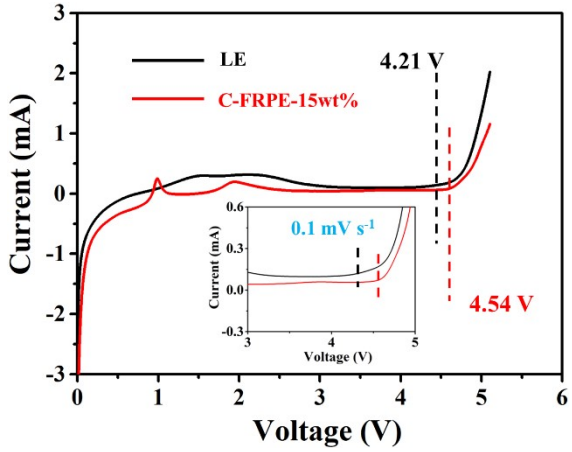

Figure S13 LSV curves of C-GPE-15 and LE

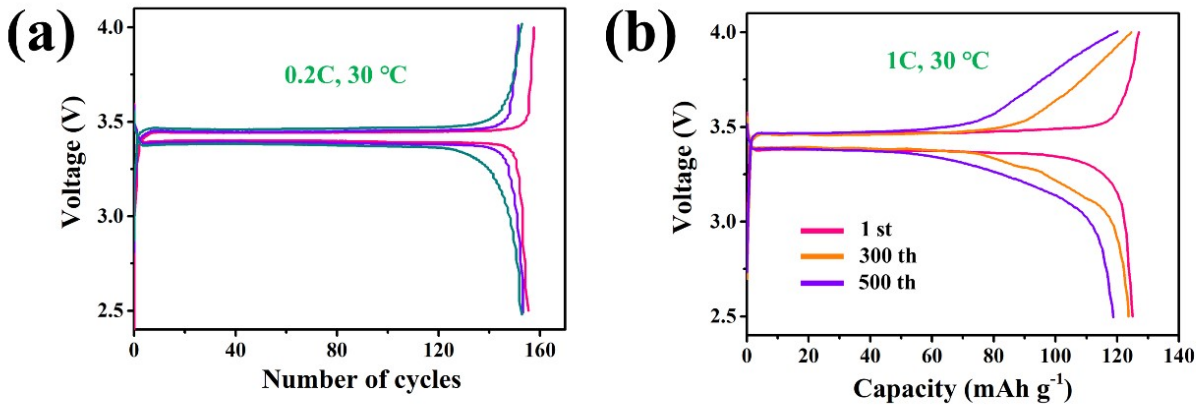

Figure S14 (a) Charge and discharge profiles of LFP/C-GPE-15/Li at 0.2 C and 1 C

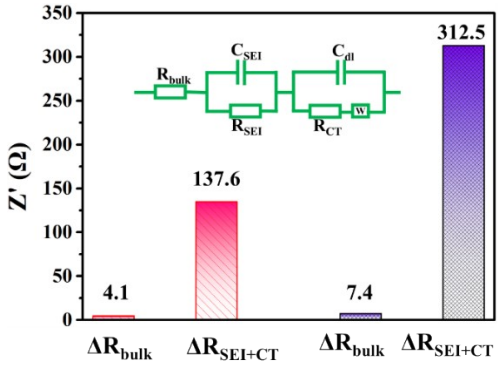

Figure S15 Impedance changes of LFP/C-GPE-15/Li and LFP/LE/Li before and after cycling at 0.5 C and 60 ℃

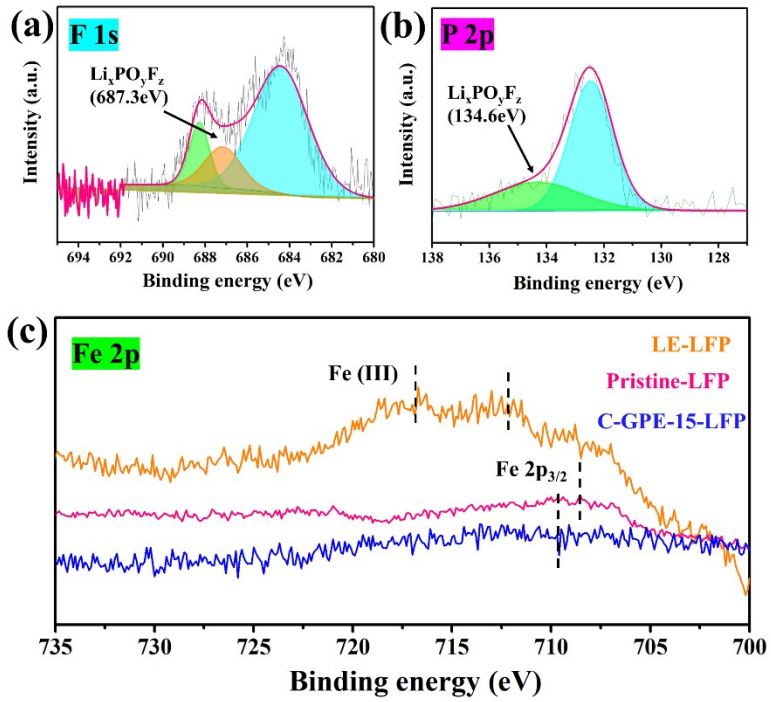

Figure S16 XPS spectrum of (a) F 1s, (b) P 2p in LFP|C-GPE-15|Li after 50 cycles at 0.2 C; (c) XPS spectrum of Fe 2p in pristine LFP, LFP in LFP|LE|Li and LFP|C-GPE-15|Li after 50 cycles at 0.2 C

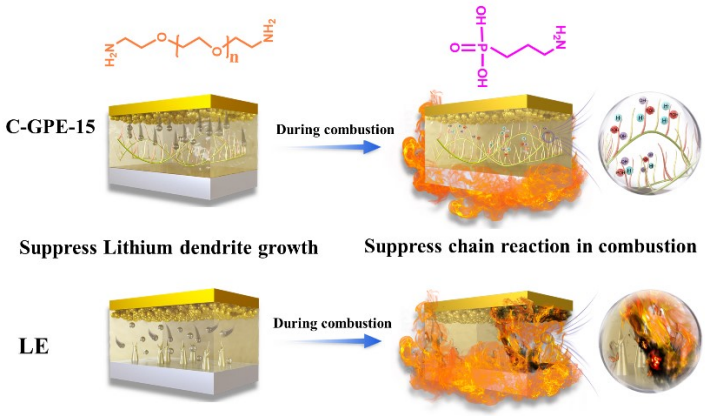

Figure S17. Schematic diagram for highly safe characteristic LMBs with C-GPE-15

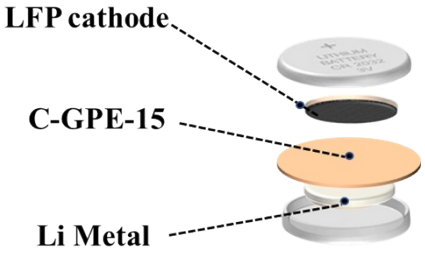

Figure S18 The assembly of Li|| C-GPE-15||LFP batteries

Table S2 Comparison of the ionic conductivity (σ) and Li^+ transference number (t_{Li+}) of C-ASPE-5/8 with those of the previously reported Flame-retardant polymer electrolytes [2-6].

	Type of electrolytes	σ/mS cm^{-1}	Cyclic performance (cycles; capacity retention rate)
C-GPE-15	GPEs	0.541	200 cycles at 0.5 C；95.2%
PEG-TEP-TiO_2	GPEs	0.251	200 cycles at 0.2 C；84%
SOTA GPEs	GPEs	/	50 cycles at 0.2 C； 96%
FRPMM-CPE	GPEs	/	240 cycles; 98%
IFR-SPE	SPEs	0.28	200 cycles; 94.8%
PEO/LiTFSI/15%ADP	SPEs	0.037	350 cycles; 92.1%

References

[1] K. Jang, H. Song, J. Park, S. Jung and D. Kim, Energy Environ. Sci., 2024, 17, 4622-4633.

[2] J. Guo, Y. Chen, Y. Xiao, C. Xi, G. Xu, B. Li, C. Yang and Y. Yu, Chemical Engineering Journal, 2021, **422**, 130526.

[3] H. Jia, H. Onishi, R. Wagner, M. Winter, and I. Cekic-Laskovic, ACS Appl. Mater. Interfaces, 2018.

[4] J. Yang, M. Zhang, Z. Chen, X. Du, S. Huang, B. Tang, T. Dong, H. Wu, Z. Yu, J. Zhang, and G. Cui. Nano Res., 2019, 12(**9**): 2230-2237.

[5] H. Li, J. Yang, S. Chen, Z. Xu, J. Wang, Y. Nuli, Y. Guo and C. Liang, Chemical Engineering Journal, 2021, **410**, 128415

[6] L. Han, C. Liao, X. Mu, N. Wu, Z. Xu, J. Wang, L. Song, Y. Kan and Y. Hu, Nano Lett. 2021, **21**,

4447–4453.